

Energy & Environmental Science

Accepted Manuscript



This is an *Accepted Manuscript*, which has been through the Royal Society of Chemistry peer review process and has been accepted for publication.

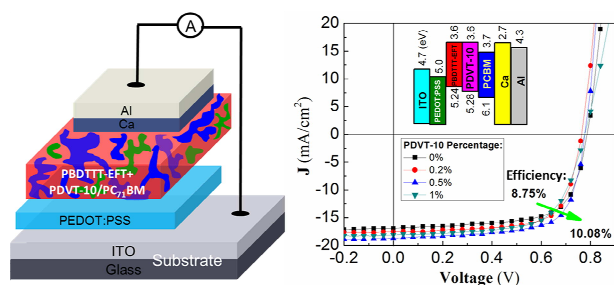
Accepted Manuscripts are published online shortly after acceptance, before technical editing, formatting and proof reading. Using this free service, authors can make their results available to the community, in citable form, before we publish the edited article. We will replace this *Accepted Manuscript* with the edited and formatted *Advance Article* as soon as it is available.

You can find more information about *Accepted Manuscripts* in the [Information for Authors](#).

Please note that technical editing may introduce minor changes to the text and/or graphics, which may alter content. The journal's standard [Terms & Conditions](#) and the [Ethical guidelines](#) still apply. In no event shall the Royal Society of Chemistry be held responsible for any errors or omissions in this *Accepted Manuscript* or any consequences arising from the use of any information it contains.

COMMUNICATION

A table of contents entry:



The efficiencies of organic solar cells are substantially improved by introducing suitable high mobility conjugated polymers as additives.

A brief paragraph (no more than 200 words) that puts your work into the broader context, highlighting the main advances and their impact on energy and environmental science. This text will be published as a separate section within your article.

Organic solar cells have attracted much attention recently for their easy fabrication, low cost, solution processability and mechanical flexible. However, the efficiencies of organic solar cells are still much lower than that of a commercialized solar cell. Therefore, effective techniques for improving the efficiencies of organic solar cells are urgently needed. Here, we report a novel technique for improving the efficiencies of organic solar cells by introducing a high-mobility conjugated polymer as an additive for the first time. Under optimum conditions, the efficiencies of one type of organic solar cells can be improved from 8.75% to 10.08%, which is mainly attributed to the improved hole mobilities in the devices. We also find that, besides the high hole mobility, the band structure of the conjugated polymer is critical to the efficiency enhancement because the energy levels of the molecular orbitals can influence carrier recombination and lifetimes in the devices. The technique is convenient and cost effective since there are plenty of choices in using high-mobility polymers. This work paves a way for realizing high-performance organic solar cells in the near future.

COMMUNICATION

Enhanced Efficiency in Polymer Solar Cells by Adding a High-Mobility Conjugated Polymer

Cite this: DOI: 10.1039/x0xx00000x

Shenghua Liu,^a Peng You,^a Jinhua Li,^a Jun Li^e Chun-Sing Lee,^d Beng S. Ong,^c Charles Surya,^b and Feng Yan^{*a}

Received 00th January 2015,

Accepted 00th January 2015

DOI: 10.1039/x0xx00000x

www.rsc.org/

The performance of organic solar cells is substantially enhanced by introducing high-mobility conjugate polymers as an additive for the first time. The most pronounced effect is observed in one type of devices with the average power conversion efficiencies increased from 8.75% to 10.08% after the addition of a high-mobility polymer for only 0.5 weight percent in the active layers, which is mainly attributed to the increased hole mobility and carrier lifetime in the devices. Besides the hole mobility, the energy band structure of the additive is also found to be critical to the enhancement of the device performance. This work demonstrates a novel approach for improving the efficiencies of organic solar cells.

Organic photovoltaics (OPVs) have attracted much attention recently in virtue of their advantages, including light weight, low cost, mechanical flexibility and easy fabrication, over conventional solar cells.¹⁻⁵ One of the most concerned and critical issue in OPVs for commercialization is the power conversion efficiencies (PCEs) of the devices. Nowadays, lots of strategies have been developed to enhance the PCEs of OPVs based on different principles, such as the introduction of buffer layers,⁶⁻⁹ additives,¹⁰⁻¹⁴ nanoparticles with surface plasmon resonance effect,¹⁵⁻¹⁹ and tandem architecture,²⁰⁻²² etc. with a view to enhancing the light absorption and tuning the energy band structure of the devices.

One limitation in many high-efficiency OPVs, such as the representative devices based on polythieno[3,4-b]-thiophene/benzodithiophene (PTB7) and [6,6]-phenyl C₇₁-butyric acid methyl ester (PC₇₁BM),^{23,24} is the low hole mobilities in the devices, which prohibit the further improvement of the device performance. A reasonable approach to overcome this limitation is to introduce high-mobility materials as additives in the active layers. For example, carbon nanotubes were added in OPVs to facilitate charge transport and improved PCEs of the devices successfully.^{25,26} Considering some high-mobility polymers recently reported exhibiting carrier mobilities several orders of magnitude higher than that in OPVs, similar effect would be expected if the high-

mobility polymers were added in the active layers, which however has never been reported before. On the other hand, it has been recognized that ternary blend solar cells with two donor materials may have higher efficiencies due to enhanced light absorption, improved charge separation and carrier transport, and suppressed carrier recombination for the cascaded band structure in the active layers.²⁷⁻³⁰ Therefore, the addition of another high-mobility polymer with a suitable band structure in an OPV would be a promising strategy for improving the device efficiency.

In this paper, we try to improve the PCEs of OPVs by adding suitable high-mobility polymers, including alkyldiketopyrrolo-pyrrole and dithienylthieno[3,2-b]thiophene (DPP-DTT) and poly[2,5-bis(alkyl)pyrrolo[3,4-c] pyrrole-1,4(2H,5H)-dione-alt-5,5'-di(thiophene-2-yl)-2,2'-(E)-2 -(2-(thiophen-2-yl)vinyl) thiophene] (PDVT-10),^{31,32} which have the hole mobilities (~10 cm²/Vs) about four orders of magnitude higher than that in conventional OPVs. We find that a little amount of DPP-DTT addition (1 wt.%) can lead to a significant increase of the PCE of PTB7/PC₇₁BM-based OPVs from 7.58% to 8.33%, which is mainly due to the remarkable increase in the hole mobilities of the devices. In addition, DPP-DTT could enhance the light absorption of the OPVs in the wavelength region longer than 700 nm, as indicated by the external quantum efficiencies (EQEs) of the devices and the UV-visible absorption spectra of the DPP-DTT polymer. Similarly, the average efficiency of the OPVs based on poly[4,8-bis(5-(2-ethylhexyl)thiophen-2-yl)-benzo[1,2-b;4,5-b']dithiophene-2,6-diyl-alt-(4-(2-ethylhexyl)-3-fluorothieno[3,4-b]thiophene-)-2-carboxylate-2-6-diyl] (PBDTTT-EFT) and PC₇₁BM can be improved from 8.75% to 10.08% by adding the high mobility polymer PDVT-10.³³ The key issue in choosing a suitable high-mobility polymer here is to have the similar HOMO levels of the high-mobility polymer and the polymer donor in OPVs, which can lead to a pronounced enhancement of the hole mobility in the devices.

The experimental section is presented in the supplementary information. We firstly fabricated ternary OPVs based on PTB7+DPP-DTT/PC₇₁BM with the device structure shown in Figure 1 by solution process on indium tin oxide (ITO) glass, in which DPP-DTT was added in the active layer only for low

percentage. The high-mobility DPP-DTT polymer contains a conjugated acceptor moiety and a comparatively stronger donor moiety.³¹ The corresponding energy diagram of the device is shown in Figure 2a. All of the energy levels of PTB7, PC₇₁BM and DPP-DTT chosen from literature were determined by the cyclic voltammetry method.^{21, 31} It is notable that the highest occupied molecular orbital (HOMO) levels of PTB7 and DPP-DTT are very close and the energy difference is only ~50mV, which is close to the product of the Boltzmann constant k and the room temperature T ($kT \sim 26\text{mV}$, for $T=300\text{K}$). On the other hand, the distribution of the density of states of the HOMO level in a conjugated polymer is normally within 100mV.³⁴ So holes can transport in the mixture of the two polymers.

The light absorption peak of DPP-DTT is around 825nm while PTB7/PC₇₁BM can absorb light only below 750nm (See supplementary information, **Figure S1**). The light absorption in the near infrared region from 750nm to 900nm of PTB7/PC₇₁BM added with DPP-DTT increases with the increasing DPP-DTT percentage. Therefore, PTB7 and DPP-DTT fit very well in terms of their complementary light absorption.

Figure 2a shows the current density versus bias voltage (J-V) curves of the OPVs added with DPP-DTT with different percentage. Here, the active layer thicknesses of all OPVs were controlled to be ~90nm, which is the optimum thickness of this type of OPVs (See supplementary information, **Figure S2**).²⁴ The weight ratio of the p-type (i.e. PTB7+DPP-DTT) to n-type (i.e. PC₇₁BM) semiconductors was kept to be 1:1.5. The weight percentages of the added DPP-DTT relative to PTB7 were controlled to be 0.5%, 1%, 2.5% and 5%, respectively. To evaluate the effect of the additive, PTB7/PC₇₁BM and DPP-DTT/PC₇₁BM binary control devices were also fabricated and characterized at the same conditions. For each condition, at least three devices were fabricated to calculate the average PCEs. Detailed photovoltaic performance including open-circuit voltage (V_{oc}), short circuit current (J_{sc}), fill factor (FF), average PCE and PCE enhancement relative to the PTB7/PC₇₁BM control devices are summarized in Figure 2b and 2c and **Table S1** in the supplementary information.

The PTB7/PC₇₁BM control devices give an average V_{oc} of 0.745 V, J_{sc} of 14.4 mA/cm², FF of 71.1% and an average PCE of 7.58%, which are comparable with the performance in literature.²³ After being added with 0.5 wt.% DPP-DTT polymer in the photoactive layer, the devices show the average V_{oc} , J_{sc} , and FF of 0.740V, 16.0 mA/cm² and 68.2%, respectively, which result in an obvious increase of the average PCE to 8.08%. For the devices added with 1.0 wt.% DPP-DTT, more significant improvement of PCEs (8.33±0.13%) can be observed, resulted from the increases in J_{sc} (15.8 mA/cm²) and V_{oc} (0.762V). It is notable that the PCE enhancement relative to the control devices is 9.9±1.8%. However, further increase of the addition amount of DPP-DTT to 2.5 wt.% and 5 wt.% lead to the decrease of PCEs to around 7.79% and 7.42% in average, respectively, mainly due to the obvious decrease in J_{sc} of the devices. The decreasing efficiency with the increase of DPP-DTT percentage when it is higher than 1% is also consistent with the performance of the control device based on DPP-DTT/PC₇₁BM, which shows the PCE of only 2.3% presented in Figure 2a. Therefore, the optimum addition amount of DPP-DTT in the ternary OPVs is around 1 wt.%. Compared with the other ternary OPVs reported recently,^{27-30, 35} the DPP-DTT

additive shows a pronounced effect at the weight percentage of only 1 wt.%, which is much more effective in modulating the efficiency of OPVs than other materials.

External quantum efficiency (EQE) measurements of the OPVs were subsequently conducted to better illuminate the enhancement of the device performance. As shown in Figure 2d, the control device without the additive exhibits the maximum EQE of 63.2%, while the others added with 0.5 wt.% and 1 wt.% DPP-DTT into the active layers show the maximum EQEs of 67.6% and 68.0%, respectively. The improvement of EQE can be observed in the whole characterized wavelength region. However, more addition of DPP-DTT (2.5 wt.% and 5 wt.%) inversely decrease EQE in the wavelength region between 350nm and 700nm and the control device of DPP-DTT/PC₇₁BM shows the lowest EQE in this region.

The enhancement of EQE beyond the wavelength of 750 nm, as illustrated in the inset of Figure 2d, can be ascribed to the light absorption of DPP-DTT in this wavelength region. So it is reasonable to find that the EQE value in this region increases with the increasing additive amount. But this effect is obviously not the main reason for the increase of PCE in the devices. Besides light absorption, exciton dissociation and carrier recombination/transport in the active layers are also critical issues to the performance of OPVs, which will be studied next to better understand the PCE enhancement due to DPP-DTT.

Firstly, to characterize the influence of DPP-DTT on carrier transport in the OPVs, hole-only devices with the device structure of ITO/PEDOT:PSS/blend layer/Au and electron-only devices with the structure ITO/ZnO/blend layer/Al were prepared (See supplementary information). To avoid leakage induced by impurities or pinholes in the active layers, the thicknesses of the blend layers were controlled to be 250~300nm. As shown in Figure 3a and 3b, electron and hole currents versus bias voltage were characterized in the devices with different percentage of DPP-DTT. The curves can be fitted very well with the space charge limited currents (SCLCs) given by the Murgatroyd equation.^{36,37} As shown in Figure 3c, the calculated electron and hole mobilities change with the amount of DPP-DTT. It is interesting to notice that the hole mobility increases with the increase of the DPP-DTT percentage, which is reasonable because of the high hole mobility of DPP-DTT. However, the electron mobility decreases with the increase of DPP-DTT amount and shows the similar value of hole mobility when the DPP-DTT percentage is around 1wt.%. From device physics point of view, the equivalent electron and hole mobilities are favourable for charge transport in the OPVs, which is one of the main reasons for the highest PCE obtained at 1wt.% DPP-DTT addition.^{30, 38}

To better understand the decrease of electron mobility with the addition of DPP-DTT, the blend films with the same thickness of around 300nm were characterized by Grazing Incidence X-Ray Diffraction (GIXD, Regaku 9KW SmartLAB).³⁹ As shown in Figure 4a, the out-of-plane diffraction peaks for pure PC₇₁BM and PTB7 films can be observed. The PTB7 film shows a peak at $q=1.6 \text{ \AA}^{-1}$, corresponding to the lattice plane (010).²⁷ The amorphous PC₇₁BM shows three broad peaks ($q=0.70, 1.3$ and 1.9 \AA^{-1}) originated from the superposition of several peaks for different lattice planes.²⁸ In the following discussion, the main peak at $q=1.3 \text{ \AA}^{-1}$ is taken as a measure for the crystallization degree of PC₇₁BM. As shown in **Figure S3**

in supplementary information, both peaks can be fitted very well with the Lorentz function. The peak widths w are 0.252 \AA^{-1} and 0.357 \AA^{-1} for PC₇₁BM ($q=1.3 \text{ \AA}^{-1}$) and PTB7 ($q=1.6 \text{ \AA}^{-1}$), respectively.

Figure 4b shows the diffraction peaks of the blend films with different weight percentage of DPP-DTT. We fitted the GIXD curves with the three Lorentz peaks (two for PC₇₁BM and one for PTB7) in the region $1.0 \text{ \AA}^{-1} \leq q \leq 2.1 \text{ \AA}^{-1}$, as shown in **Figure S4** in the supplementary information. The peak width of PC₇₁BM at $q=1.3 \text{ \AA}^{-1}$ shown in Figure 4c increases with the increasing addition of DPP-DTT and the DPP-DTT/PC₇₁BM film shows the biggest width of 0.482 \AA^{-1} . So the addition of DPP-DTT can damage the crystallinity of PC₇₁BM and consequently decrease the electron mobility in the device.

Moreover, we measured the surface roughness of the PTB7+DPP-DTT/PC₇₁BM films with different addition levels prepared at the same conditions of OPVs. As shown in **Figure S5** and **Table S2** in the supplementary information, the surface roughness decreases with the increase of addition level, indicating that DPP-DTT can inhibit the crystallization in the active layers, being consistent with the morphology change observed in other ternary OPVs.^{30,40}

Secondly, the donor/acceptor interface properties are critical to exciton dissociation and carrier recombination in OPVs. It has been reported that the DPP-DTT/PC₇₁BM interface is not ideal for exciton dissociation due to the small energy offset between their lowest unoccupied molecular orbital (LUMO) levels.⁴¹ As shown in Figure 2a, the LUMO levels for DPP-DTT and PC₇₁BM are 3.5eV and 3.7eV,^{21,31} respectively. The energy difference between the two LUMO levels is about 0.2eV, which is lower than the required value (normally 0.3~0.4eV) for efficient exciton dissociation at an organic heterojunction.⁴¹ The poor exciton dissociation can also be reflected by the low EQE of DPP-DTT/PC₇₁BM control device shown in Figure 2d.

On the other hand, the ternary OPVs have a cascaded band structure, which is favourable for prohibiting carrier recombination in the devices, as discussed, for example, by Lu et al.²⁷ To characterize the geminate carrier recombination process at the donor/acceptor interfaced, the impedance of the OPVs were measured by an impedance analyzer (HP4294) under different bias voltages in the dark (See supplementary information, Figure S6) and the carrier lifetime can be decided from the top position of each Nyquist plot of the impedance.⁴² Figure 4d shows the carrier lifetime as a function of bias voltage for different DPP-DTT addition level. The carrier lifetime decreases with the increase of bias voltage due to the increasing carrier density at the heterojunction.^{37, 43} For different samples at the same bias voltage, the longest carrier lifetime appears at the DPP-DTT addition of 1wt.%. With more addition of DPP-DTT, the carrier lifetime is decreased, which however is not expected in the devices with the cascaded band structure. It is notable that the carrier lifetime in DPP-DTT/PC₇₁BM is much shorter than that in PTB7/PC₇₁BM at the same bias voltage. Therefore the carriers can more easily recombine at the interface of DPP-DTT/PC₇₁BM, which is the main reason for the decreased carrier lifetime with the increase of DPP-DTT addition when it is higher than 1wt.%. Considering that the V_{oc} of an OPV decreases with the increase of the carrier recombination rate at the heterojunction,^{43,44} the longest carrier lifetime at the DPP-DTT addition level of 1wt.%

can also be confirmed by the highest V_{oc} at this addition level shown in Figure 2b. Therefore, DPP-DTT can influence the carrier recombination process in the ternary OPVs by two ways. One is to prohibit the recombination of free electrons and holes due to the cascaded band structure and another one is to accelerate the carrier recombination at the DPP-DTT/PC₇₁BM interface. The compromise of the two effects results in the optimum amount of the additive at ~1wt.%.

To check the effect of other high-mobility polymers, we introduced another DPP-based high-mobility copolymer PDVT-10 in PTB7/PC₇₁BM-based OPVs. PDVT-10 shows high hole mobilities up to $8.2 \text{ cm}^2/\text{Vs}$,³² being comparable to that of DPP-DTT. However, the HOMO level of PDVT-10 is 5.28 eV, which is ~130mV higher than that of PTB7.³² The band structure of the ternary OPV is shown in the inset of Figure S7 in the supplementary information. We find that the PCEs of the devices decrease with the increasing amount of PDVT-10 and a little efficiency enhancement can be observed only at the addition percentage of 0.5 wt.%, as shown in Figure S7 in the supplementary information. To better understand the effect, we have characterized the carrier mobilities in the films with different addition percentage (0.5%, 1%, %, 5%) by SCLC measurements. As shown in Figure S8 in the supplementary information, the hole mobility has little change while the electron mobility decreases rapidly with the increase of addition amount. It is notable that the HOMO levels of PTB7 and PDVT-10 have the energy difference of about 130mV. Therefore, holes in PDVT-10 tend to move to PTB7 due to decreased energies and thus the hole mobility in the blend film cannot be increased by PDVT-10 for too much value. On the other hand, electron mobilities in the OPVs are decreased by the additive. So the addition of PDVT-10 decreases the efficiency of the OPVs monotonically with the addition amount.

To further confirm the generality of the approach, another type of OPV based on PBDTTT-EFT/PC₇₁BM was fabricated with the addition of the high mobility polymers DPP-DTT and PDVT-10. PBDTTT-EFT has a broader light absorption region than PTB7 and its HOMO level is 5.24 eV.⁴⁵ So the HOMO levels of both PDVT-10 and DPP-DTT are very close to that of PBDTTT-EFT. Figure 5a and 5b show the J-V curves and the PCEs of the OPVs with the addition of DPP-DTT of different amount. It is interesting to note that DPP-DTT cannot induce any improvement of the device efficiency although the short circuit current is improved. As shown in the inset of Figure 5a, the addition of DPP-DTT in the PBDTTT-EFT/PC₇₁BM blend films cannot form a cascaded band structure, which is the major reason for the lack of PCE enhancement in the devices.

Figure 5c and 5d show the J-V curves and the PCEs of the OPVs with the addition of PDVT-10 of different percentage. The detailed data are shown in **Table S3** in the supplementary information. A dramatic enhancement in the PCEs of the devices can be observed and the optimum addition level of PDVT-10 is 0.5wt.%. The average PCE was enhanced from 8.75% to 10.08% at this addition level and the corresponding relative enhancement is 15.2%. The champion device shows the PCE of 10.14%, which is 15.9% higher than that of the control devices without the additive. The enhancement can be obviously attributed to the enhanced hole mobility (See the supplementary information, Figure S9) as well as the cascade band structure of the ternary OPVs shown in the inset of Figure 5c, which can prohibit geminate carrier recombination (see

Figure S10 in the supplementary information). Therefore, for PBDTTT-EFT/PC₇₁BM, PDVT-10 is a more suitable additive than DPP-DTT due to the matchable energy levels of the former one. It is notable that the device performance is very sensitive to the HOMO levels of the organic semiconductors since the HOMO energy difference of ~80 mV between DPP-DTT and PDVT-10 can lead to completely different effects.

The above explanation is based on the assumption that the energy levels in the literature are accurate enough. However, the standard errors of the energy levels are unknown and the energy levels can be finely tuned by other factors like the crystallinity and strain of the polymer films.⁴⁵ Therefore, precise simulation of the effect is not possible at this stage although all of the results can be reasonably explained.

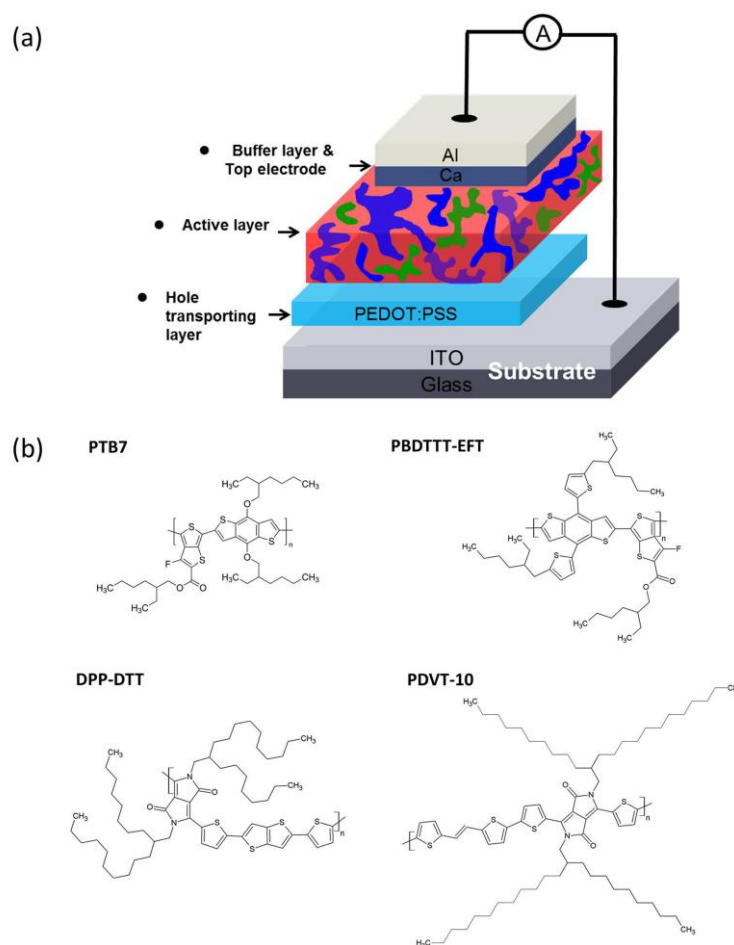


Figure 1 (a) Device architecture of the OPVs prepared in experiments; (b) Molecular structures of the used polymers, including PTB7, PBDTTT-EFT, DPP-DTT and PDVT-10.

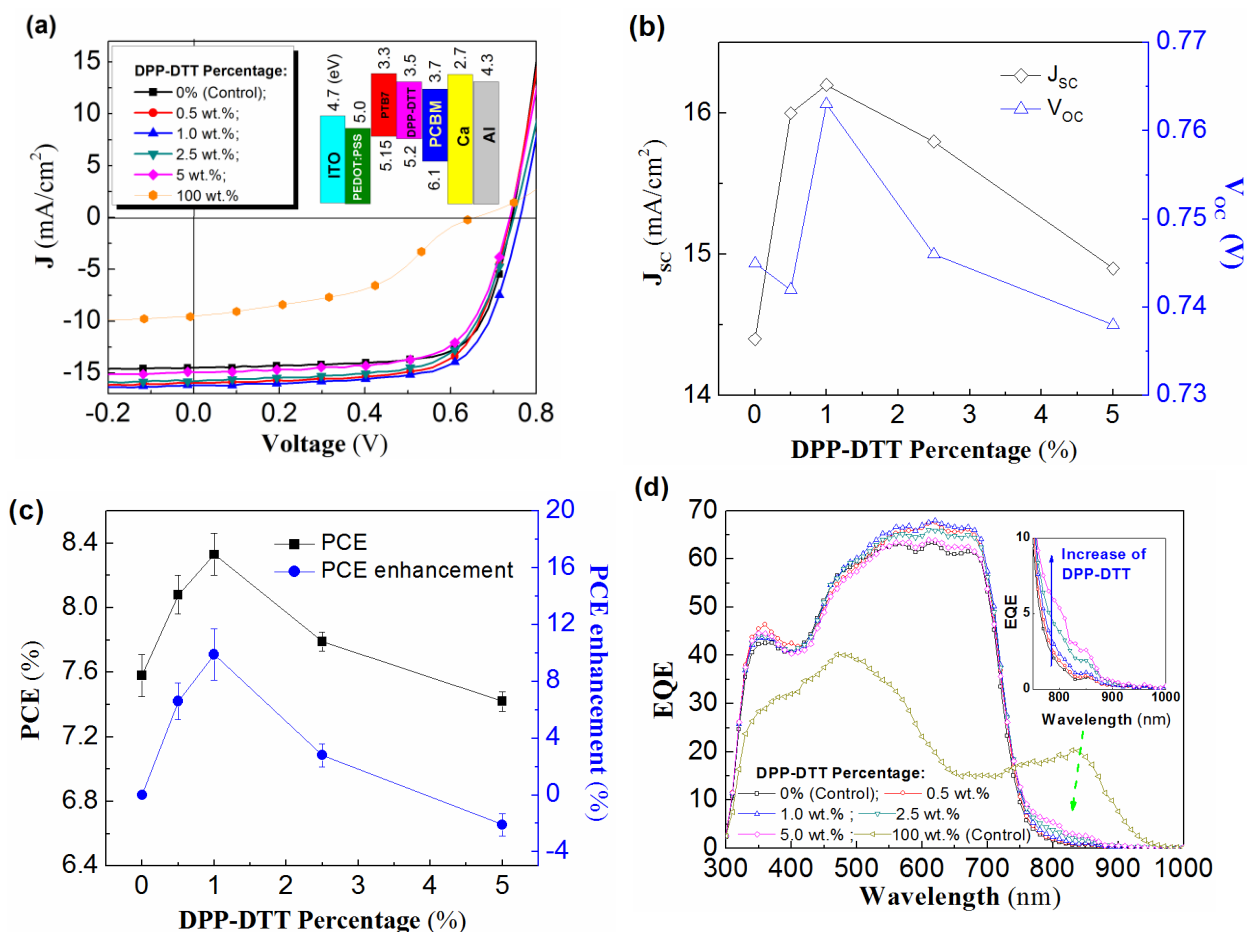


Figure 2 (a) J - V characteristics of OPVs with different addition percentage of DPP-DTT in PTB7/PC₇₁BM. The two control devices are PTB7/PC₇₁BM and DPP-DTT/PC₇₁BM OPVs. Inset: Band structure of the ternary OPVs. (b) The short circuit current density (J_{sc}) and open circuit voltage (V_{oc}) of the OPVs for different percentage of DPP-DTT. (c) The PCE and the corresponding enhancement for different DPP-DTT percentage. (d) EQEs of the OPVs with different DPP-DTT percentage. Inset: EQEs in the wavelength region from 750 to 1000nm.

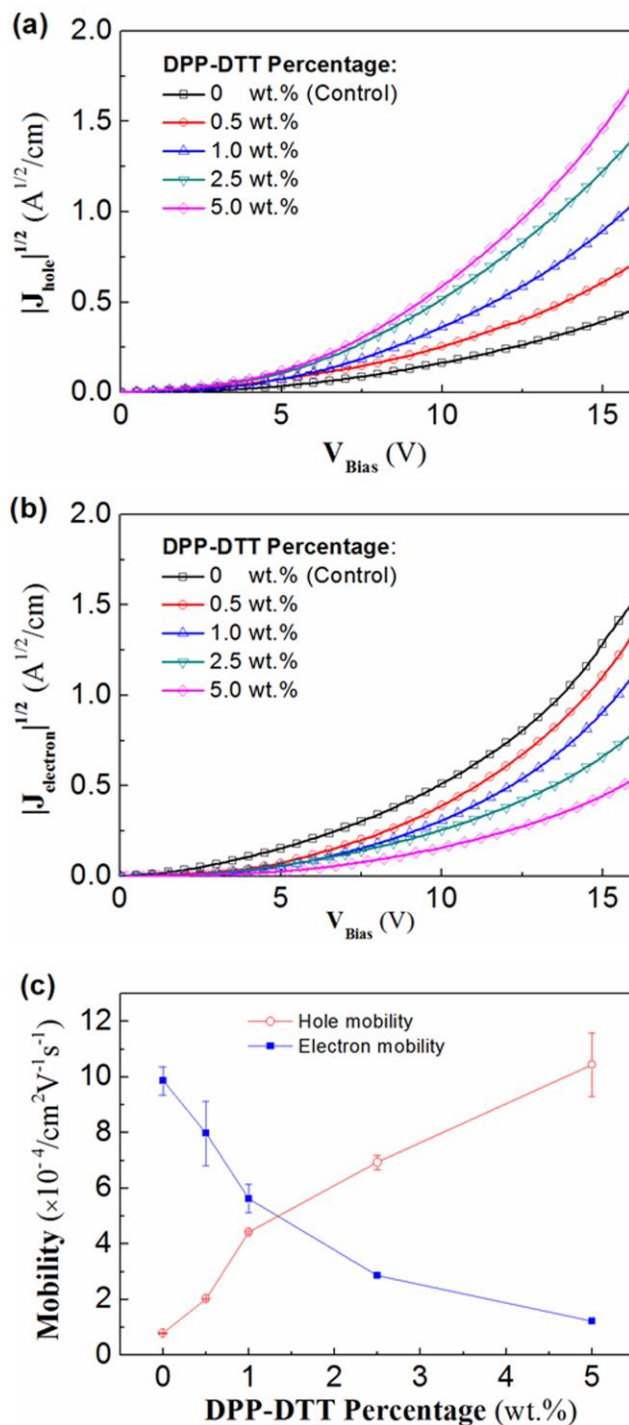


Figure 3 (a) Square root of hole current densities versus bias voltage of the ITO/PEDOT:PSS/PTB7+DPP-DTT/PC₇₁BM/Au devices with different DPP-DTT percentage. (b) Square root of electron current densities versus bias voltage of the ITO/ZnO/PTB7+DPP-DTT/PC₇₁BM/Al devices with different percentage of DPP-DTT addition. (c) Electron and hole mobilities calculated from the space charge limited currents (SCLCs) in (a) and (b).

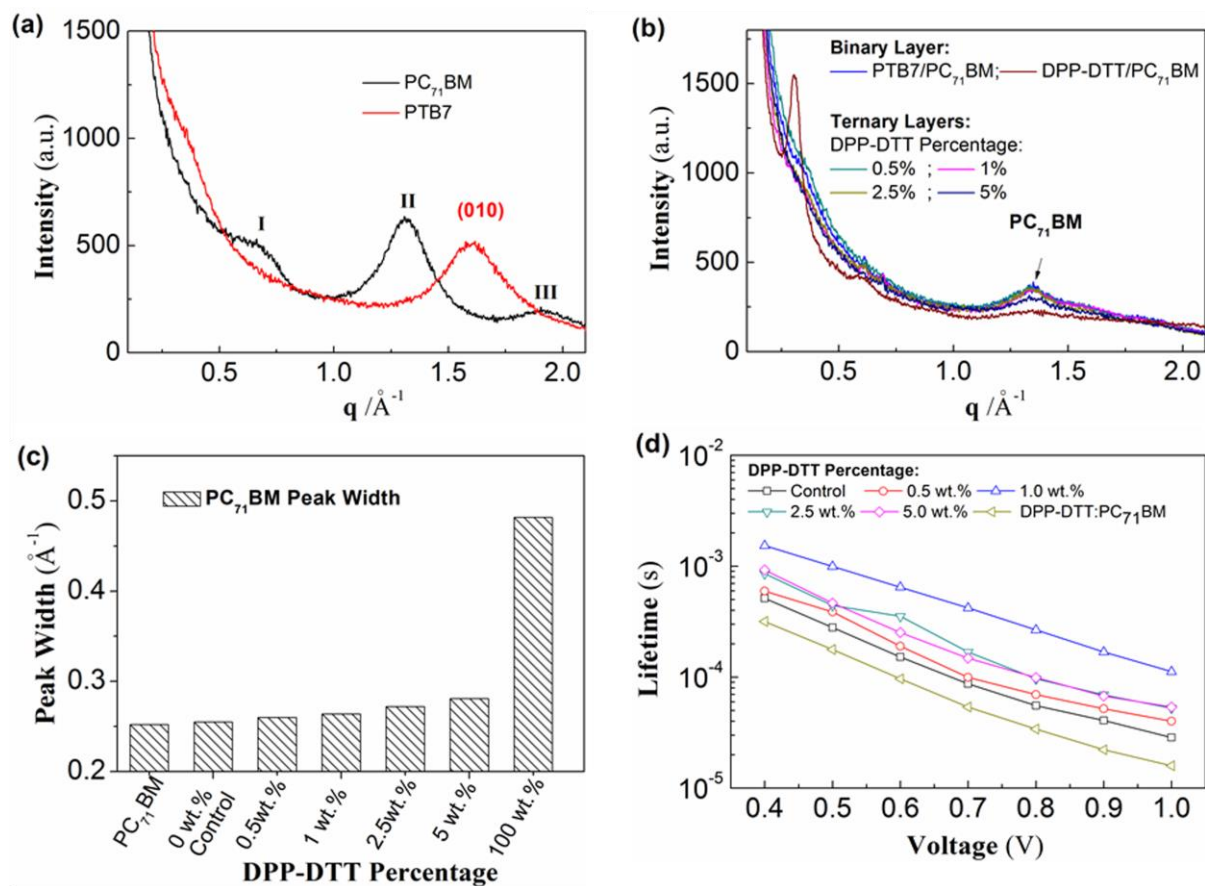


Figure 4. GIXD out-of-plane diffraction patterns of (a) a PC₇₁BM film and a PTB7 film; (b) a PTB7/PC₇₁BM film, a DPP-DTT/PC₇₁BM film and PTB7+DPP-DTT/PC₇₁BM ternary films with different DPP-DTT percentage. (c) Peak widths of the diffraction peaks at $q=1.3 \text{\AA}^{-1}$ for different DPP-DTT percentage. (d) Carrier lifetimes of different devices as functions of bias voltage.

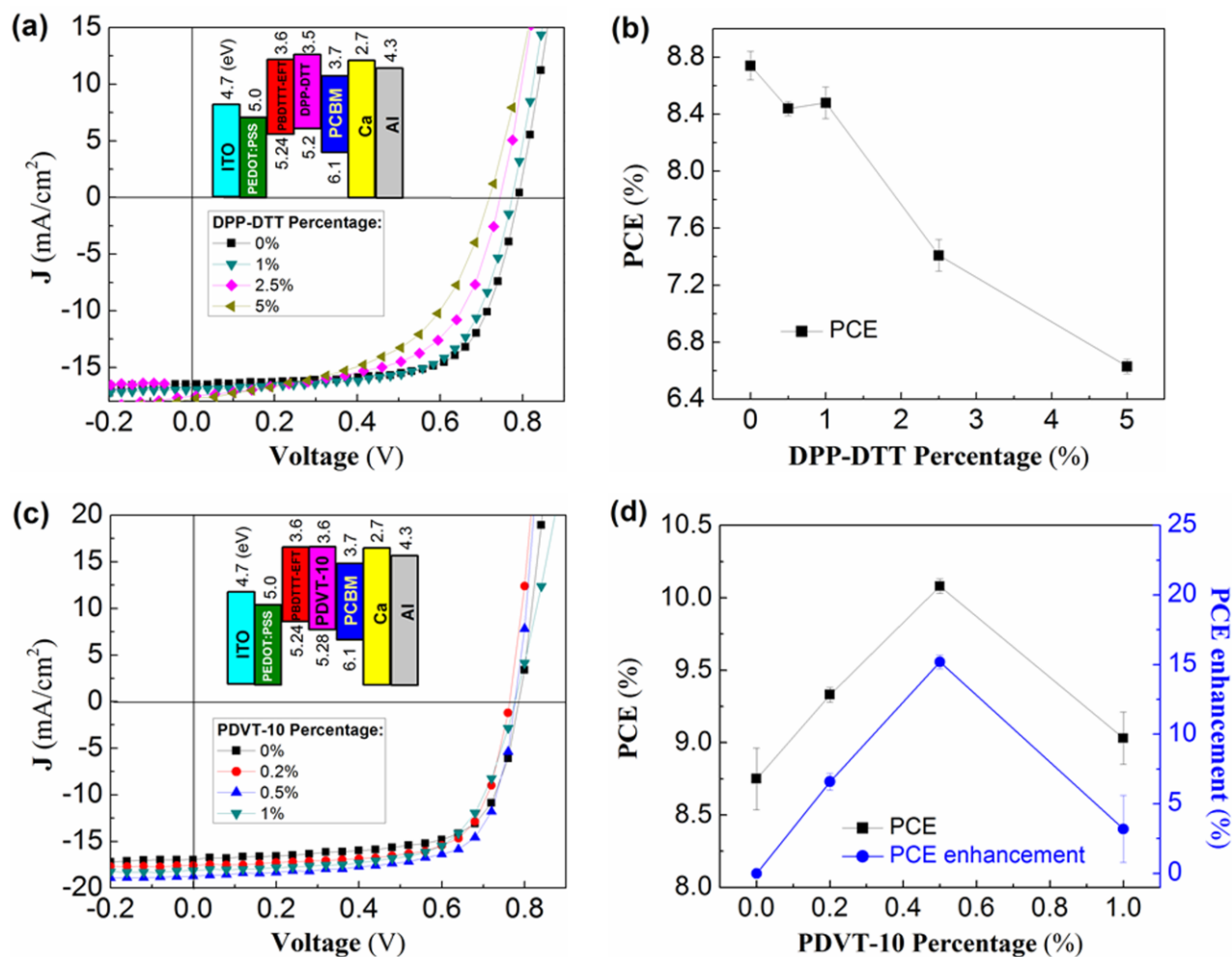


Figure 5. (a) J - V characteristics of OPVs with different addition percentage of DPP-DTT in PBDTTT-EFT/PC₇₁BM. Inset: Band structure of the ternary OPVs. (b) The PCEs for the devices based on PBDTTT-EFT/PC₇₁BM with different PDVT-10 percentage. (c) J - V characteristics of OPVs with different addition percentage of PDVT-10 in PBDTTT-EFT/PC₇₁BM. Inset: Band structure of the ternary OPVs based on PBDTTT-EFT/PDVT-10/PC₇₁BM. (d) The PCEs and the corresponding enhancement for the devices based on PBDTTT-EFT/PC₇₁BM with different PDVT-10 percentage.

Conclusions

In summary, the efficiencies of OPVs are substantially improved by adding a suitable high-mobility polymer in the active layer. For PTB7/PC₇₁BM OPVs, the average PCE is improved from 7.58% to 8.33% by adding 1 wt.% DPP-DTT and obvious improvements of EQEs over a broad wavelength range from 350 to 800 nm can be observed. For the OPVs based on PBDTTT-EFT/PC₇₁BM, PDVT-10 is a more suitable additive. The average PCE is increased from 8.75% to 10.08% at the addition level of 0.5wt.%. The significant enhancement of the PCEs can be attributed to the increased hole mobilities and carrier lifetimes in the devices. To effectively increase the hole mobilities in the devices, we find that the additive should have the similar HOMO level to that of the donor material. As evidenced in our experiments, several tens of millivolts may lead to a completely different effect. Secondly, the additive

should form a cascade band structure in the OPVs to avoid the trapping of carriers in the additive. On the other hand, the additive may induce several drawbacks, including the decreased electron mobility and lower exciton dissociation efficiency at the heterojunction. Given the aforementioned drawbacks overcome via rational material design and processing control, better effect of adding high mobility conjugated polymers in OPVs would be expected in the future. Therefore, this work demonstrates a novel approach for improving the performance of OPVs by adding high-mobility polymers.

Acknowledgements

This work is financially supported by the Research Grants Council (RGC) of Hong Kong, China (project number: T23-713/11), The Hong Kong Polytechnic University (project number: G-YM45, 1-ZV8N and 1-ZVAW), the National Natural Science Foundation of China (Project number:

51203045) and Hong Kong Baptist University Strategic Development Fund.

Notes and references

^a Department of Applied Physics, The Hong Kong Polytechnic University, Hung Hom, Kowloon, Hong Kong, China

E-mail: apafyan@polyu.edu.hk

^b Department of Electronic and Information Engineering, The Hong Kong Polytechnic University, Hung Hom, Kowloon, Hong Kong, China

^c Centre of Excellence for Organic Electronics, Institute of Creativity and Department of Chemistry, Hong Kong Baptist University, Kowloon Tong, Kowloon, Hong Kong, China

^d Center of Super-Diamond and Advanced Film (COSDAF) and Department of Physics and Materials Science, City University of Hong Kong, Hong Kong, China

^e Institute of Materials Research and Engineering, A*STAR, 3 Research Link, 117602, Singapore.

- G. Yu, J. Gao, J. C. Hummelen, F. Wudl, A. J. Heeger, *Science*, **1995**, *270*, 1789.
- L. Dou, J. You, Z. Hong, Z. Xu, G. Li, R. A. Street, Y. Yang, *Adv. Mater.*, **2013**, *25*, 6642.
- G. Li, R. Zhu, Y. Yang, *Nat. Photon.*, **2012**, *6*, 153.
- Y. F. Li, *Acc. Chem. Res.* **2012**, *45*, 723.
- Z. Liu, J. Li, F. Yan, *Adv. Mater.*, **2013**, *25*, 4296.
- S. B. Jo, J. H. Lee, M. Sim, M. Kim, J. H. Park, Y. S. Choi, Y. Kim, S.-G. Ihn, K. Cho, *Adv. Energy Mater.*, **2011**, *1*, 690.
- S.-H. Oh, S.-I. Na, J. Jo, B. Lim, D. Vak, D.-Y. Kim, *Adv. Funct. Mater.*, **2010**, *20*, 1977.
- N. Cho, H.-L. Yip, J. A. Davies, P. D. Kazarinoff, D. F. Zeigler, M. M. Durban, Y. Segawa, K. M. O'Malley, C. K. Luscombe, A. K. Y. Jen, *Adv. Energy Mater.*, **2011**, *1*, 1148.
- K. X. Steirer, P. F. Ndione, N. E. Widjonarko, M. T. Lloyd, J. Meyer, E. L. Ratcliff, A. Kahn, N. R. Armstrong, C. J. Curtis, D. S. Ginley, J. J. Berry, D. C. Olson, *Adv. Energy Mater.*, **2011**, *1*, 813.
- T. Ameri, J. Min, N. Li, F. Machui, D. Baran, M. Forster, K. J. Schottler, D. Dolfen, U. Scherf, C. J. Brabec, *Adv. Energy Mater.*, **2012**, *2*, 1198.
- T. Ameri, P. Khoram, J. Min, C. J. Brabec, *Adv. Mater.*, **2013**, *25*, 4245.
- Z. Sun, K. Xiao, J. K. Keum, X. Yu, K. Hong, J. Browning, I. N. Ivanov, J. Chen, J. Alonzo, D. Li, B. G. Sumpter, E. A. Payzant, C. M. Rouleau, D. B. Geohegan, *Adv. Mater.*, **2011**, *23*, 5529.
- B. A. Collins, Z. Li, J. R. Tumbleston, E. Gann, C. R. McNeill, H. Ade, *Adv. Energy Mater.*, **2013**, *3*, 65.
- S. J. Lou, J. M. Szarko, T. Xu, L. Yu, T. J. Marks, L. X. Chen, *J. Am. Chem. Soc.*, **2011**, *133*, 20661.
- D. H. Wang, K. H. Park, J. H. Seo, J. Seifter, J. H. Jeon, J. K. Kim, J. H. Park, O. O. Park, A. J. Heeger, *Adv. Energy Mater.*, **2011**, *1*, 766.
- L. Lu, Z. Luo, T. Xu, L. Yu, *Nano Lett.*, **2012**, *13*, 59.
- H. Choi, J.-P. Lee, S.-J. Ko, J.-W. Jung, H. Park, S. Yoo, O. Park, J.-R. Jeong, S. Park, J. Y. Kim, *Nano Lett.*, **2013**, *13*, 2204.
- S.-W. Baek, G. Park, J. Noh, C. Cho, C.-H. Lee, M.-K. Seo, H. Song, J.-Y. Lee, *ACS Nano*, **2014**, *8*, 3302.
- H. Choi, S.-J. Ko, Y. Choi, P. Joo, T. Kim, B. R. Lee, J.-W. Jung, H. J. Choi, M. Cha, J.-R. Jeong, I.-W. Hwang, M. H. Song, B.-S. Kim, J. Y. Kim, *Nat. Photon.*, **2013**, *7*, 732.
- J. You, L. Dou, K. Yoshimura, T. Kato, K. Ohya, T. Moriarty, K. Emery, C.-C. Chen, J. Gao, G. Li, Y. Yang, *Nat. Commun.*, **2013**, *4*, 1446.
- S. Sista, M.-H. Park, Z. Hong, Y. Wu, J. Hou, W. L. Kwan, G. Li, Y. Yang, *Adv. Mater.*, **2010**, *22*, 380.
- J. Y. Kim, K. Lee, N. E. Coates, D. Moses, T.-Q. Nguyen, M. Dante, A. J. Heeger, *Science*, **2007**, *317*, 222.
- Y. Liang, Z. Xu, J. Xia, S.-T. Tsai, Y. Wu, G. Li, C. Ray, L. Yu, *Adv. Mater.*, **2010**, *22*, E135.
- Z. He, C. Zhong, S. Su, M. Xu, H. Wu, Y. Cao, *Nat. Photon.*, **2012**, *6*, 591.
- J. M. Lee, J. S. Park, S. H. Lee, H. Kim, S. Yoo, S. O. Kim, *Adv. Mater.*, **2011**, *23*, 629.
- L. Lu, T. Xu, W. Chen, J. M. Lee, Z. Luo, I. H. Jung, H. I. Park, S. O. Kim, L. P. Yu, *Nano Lett.*, **2013**, *13*, 2365.
- L. Lu, T. Xu, W. Chen, E. S. Landry, and L. P. Yu, *Nat. Photon.* **2014**, *8*, 716
- F. Machui, S. Rathgeber, N. Li, T. Ameri, C. J. Brabec, *J. Mater. Chem.* **2012**, *22*, 15570.
- J. Lee, M. H. Yun, J. Kim, J. Y. Kim, C. Yang, *Macromol. rapid comm.*, **2012**, *33*, 140.
- Y. J. Zhang, D. Deng, K. Lu, J. Q. Zhang, B. Z. Xia, Y. F. Zhao, J. Fang, Z. X. Wei, *Adv. Mater.*, DOI: 10.1002/adma.201404902
- J. Li, Y. Zhao, H. S. Tan, Y. Guo, C.-A. Di, G. Yu, Y. Liu, M. Lin, S. H. Lim, Y. Zhou, H. Su, B. S. Ong, *Sci. Rep.*, **2012**, *2*, 00754.
- H. J. Chen, Y. L. Guo, G. Yu, Y. Zhao, J. Zhang, D. Gao, H. T. Liu, Y. Q. Liu, *Adv. Mater.* **2012**, *24*, 4618.
- W. C. Huang, E. Gann, L. Thomsen, C. K. Dong, Y. B. Cheng and C. R. McNeill, *Adv. Energy Mater.* DOI: 10.1002/aenm.201401259.
- H. Sirringhaus, *Adv. Mater.* **2005**, *17*, 2411.
- P. Cheng, Y. F. Li and X. W. Zhan, *Energy Environ. Sci.*, **2014**, *7*, 2005.
- P. N. Murgatroyd, *J. Phys. D* **1970**, *3*, 151.
- S. Foster, F. Deledalle, A. Mitani, T. Kimura, K.-B. Kim, T. Okachi, T. Kirchartz, J. Oguma, K. Miyake, J. R. Durrant, S. Doi, J. Nelson, *Adv. Energy Mater.* **2014**, *4*, 1400311.
- S. J. Wu, J. H. Li, Q. D. Tai and F. Yan, *J. Phys. Chem. C.*, **2010**, *114*, 21873.
- J. H. Li, Z. H. Sun, F. Yan, *Adv. Mater.* **2012**, *24*, 88.
- G. Li, V. Shrotriya, J. Huang, Y. Yao, T. Moriarty, K. Emery, Y. Yang, *Nat. Mater.*, **2005**, *4*, 864.
- J. C. Bijleveld, R. A. Melanie, M. M. Verstrijden, R. A. Wienk, J. Janssen, *J. Mater. Chem.*, **2011**, *21*, 9224.
- J. Bisquert, *J. Phys. Chem. B* **2002**, *106*, 325.
- Q. D. Tai, J. H. Li, Z. K. Liu, Z. H. Sun, X. Z. Zhao, and F. Yan, *J. Mater. Chem.*, **2011**, *21*, 6848.
- N. C. Giebink, G. P. Wiederrecht, M. R. Wasielewski, S. R. Forrest, *Phys. Rev. B* **2010**, *82*, 155305.
- S. Q. Zhang, L. Ye, W. C. Zhao, D. L. Liu, H. F. Yao and J. H. Hou, *Macromolecules*, **2014**, *47*, 4653.
- Z. H. Sun, J. H. Li, C. M. Liu, S. H. Yang and F. Yan, *Adv. Mater.* **2011**, *23*, 3648.